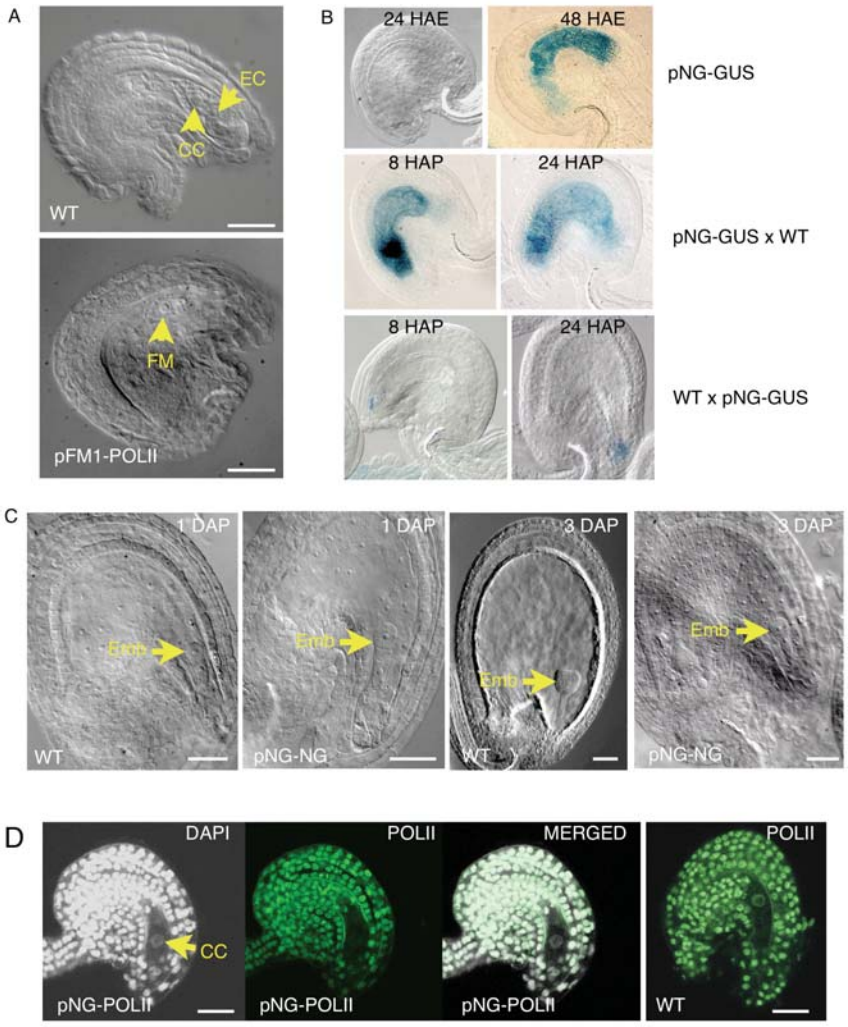

Supplemental Figure 1: Control lines showing effective RNA interference in ovules and seeds

(A) Wild type (WT) mature ovule (top) and ovule from transgenic plants containing a pFM1-driven RNAi construct targeting POLII (bottom), with an arrested functional megaspore (FM); CC: central cell, EC: egg cell.

(B) Histochemical detection of GUS reporter gene expression in reciprocal crosses between pNG-GUS and wild type (WT) plants. Before fertilization, promoter activity is detected in the embryo sac only once the ovule is mature (pNG-GUS 48 hours after emasculation (HAE) compared to 24 HAE); after fertilization, promoter activity is detected maternally in the early embryo and endosperm, paternal expression contributing only for a minor part at the base of suspensor probably marking pollen tube discharge point (pNG is strongly active in pollen and pollen tubes) (reciprocal crosses 8 HAP and 24 HAP, hand-pollination performed 40 HAE).

(C) Wild type (WT) and pNG-NG RNAi lines 1 DAP and 3 DAP. WT seed 1 DAP shows a one-cell embryo (arrow) associated with a syncytial endosperm; mutant seed 3 DAP carrying a pNG-NG RNAi construct targeting NG under its own promoter sequence shows an arrested one-cell embryo (arrow) surrounded by a much older, cellularized endosperm.

(D) Immunolocalization of POLII antibody (H5) in wild type (WT) and pNG-POLII RNAi lines; CC: central cell; projection of consecutive optical sections.

Scale bar: 10µm.

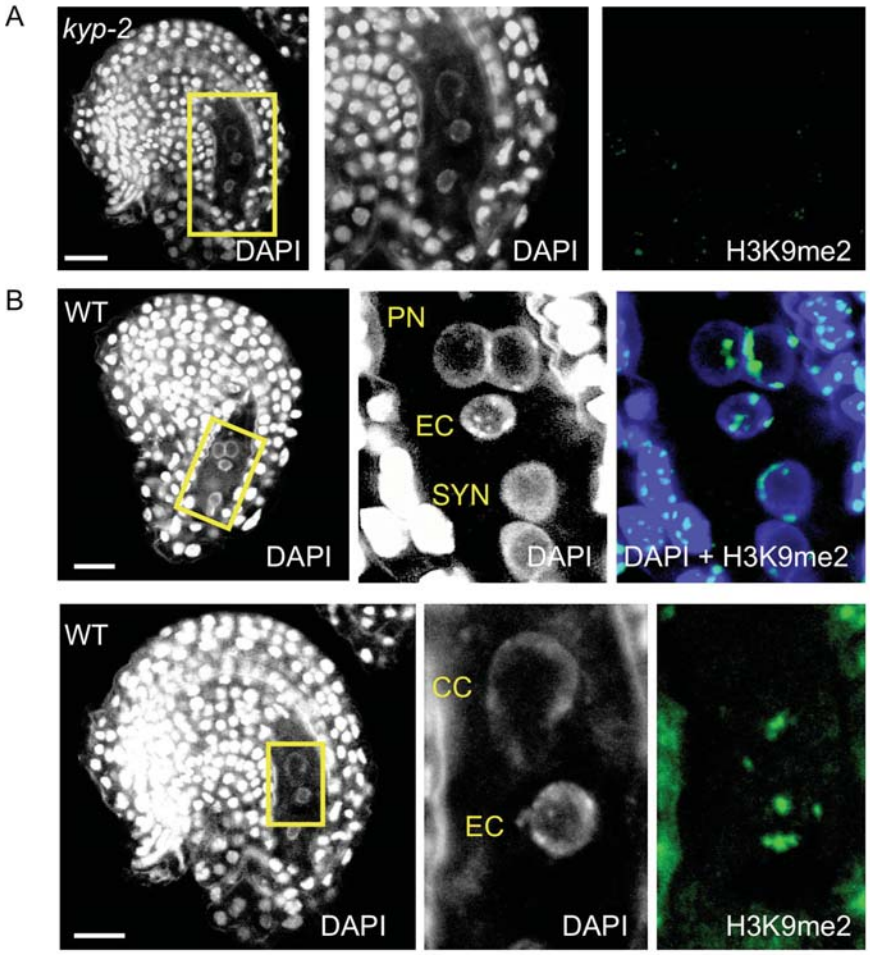

Supplemental Figure 2: Dynamic of H3K9me2 during the differentiation of the central cell.

(A) *kyp-2* mutant seed stained with DAPI (left), close up as defined by the yellow box (center) and H3K9me2 (right); projection of consecutive optical sections. The absence of signal confirms the specificity of the antibody.

(B) Top: immature ovule immediately before the fusion of the polar nuclei; single optical section of the whole ovule stained with DAPI (left); close-up on DAPI (center) and overlay of DAPI (blue) and H3K9me2 (green) signals (right); projection of consecutive optical sections. Bottom: mature ovule; DAPI (white) and H3K9me2 (green) signals; projection of consecutive optical sections. While chromocenters and associated H3K9me2 signals are clearly visible in both cell types until the fusion of the polar nuclei, the association is lost at later stages in the central cell. Chromocenters become difficult to detect with DAPI, and H3K9me2 are significantly reduced in the central cell. SYN: synergids; EC: egg cell; PN: polar nuclei; CC: central cell.

Scale bar: 10µm.

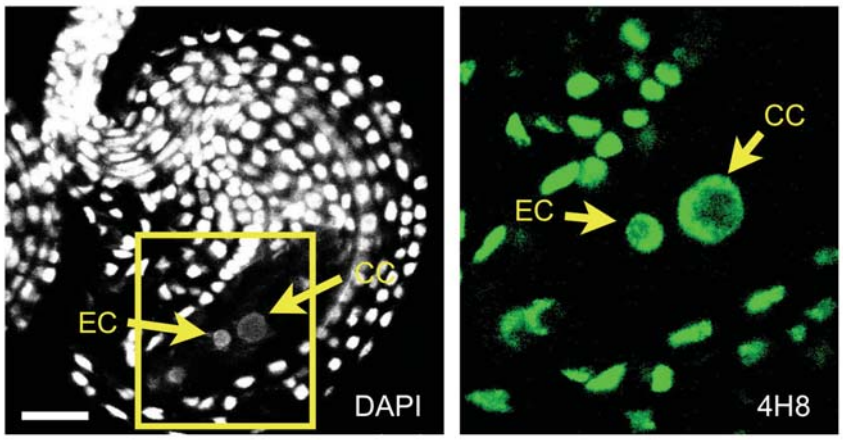

Supplemental Figure 3: Detection of POLII in the mature ovule.

Mature ovule prior to fertilization stained with DAPI (white, single optical section) and 4H8 (green, projection of consecutive optical sections); 4H8 specifically recognizes the heptamer repeats of the C-terminal domain of the main subunit of POLII, and is independent of the phosphorylation status of the serine residues in position 2 and 5. It is thus a general marker of POLII, and the results indicate that the protein is detected, at comparable levels, in both the egg cell and the central cell; EC: egg cell; CC: central cell.

Scale bar: 10µm.

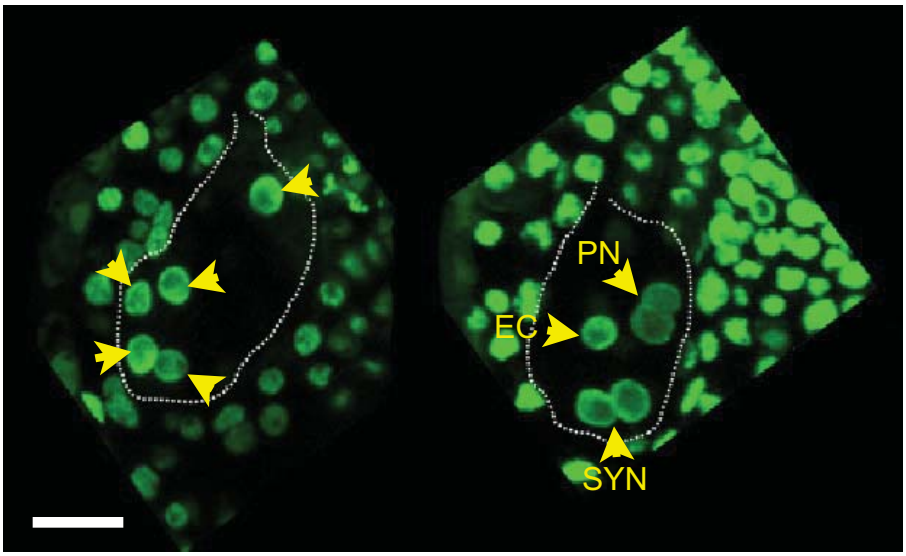

Supplemental Figure 4: TFL2 distribution during ovule development.

Ovules expressing a pTFL2: TFL2-GFP transgene; for all images, projection of consecutive optical sections showing the nuclei within the embryo sac (delimitated by the dash line) and the ovule integuments. EC: egg cell; PN: polar nuclei; SYN: synergids.

(A) Ovule prior to cellularization of the gametophyte, illustrating comparable distribution of the GFP signal in all gametophytic nuclei (arrows).

(B) Ovule following cellularization, but before fusion of the polar nuclei.

Scale bars: 10µm.

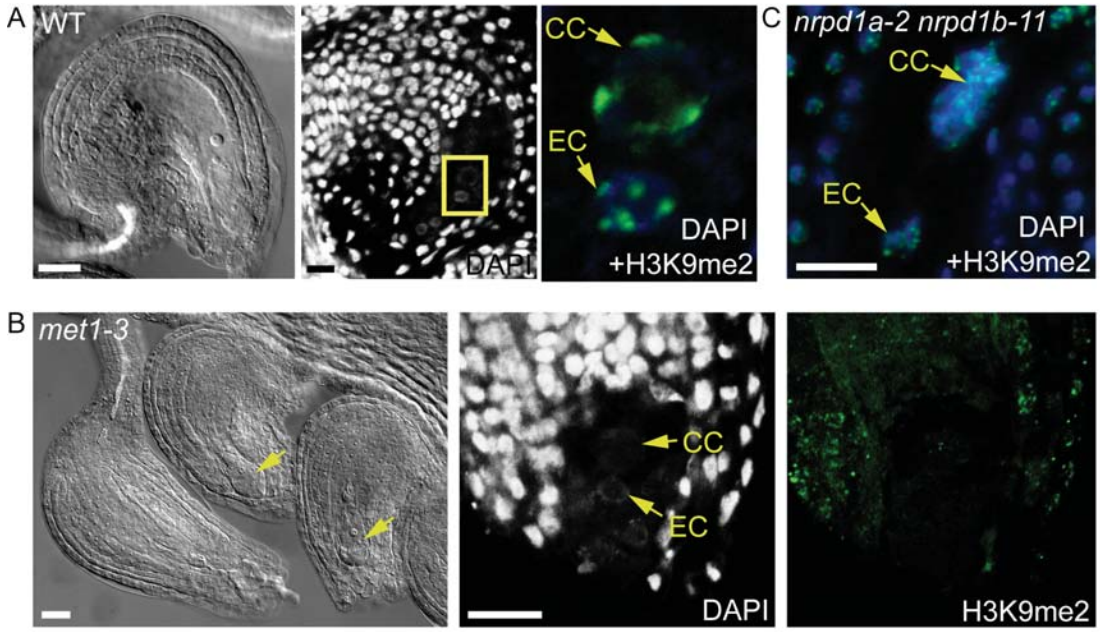

Supplemental Figure 5: H3K9me2 patterns in *met1-3* and *nrpd1a-2 nrpd1b-11* embryo sacs.

(A) Wild type (WT) ovules. Whole-mount clearing (left), whole ovule stained with DAPI (center) and close-up showing overlay of DAPI (blue) and H3K9me2 (green) signals (right).

(B) *met1-3* ovules. Whole-mount clearing (left): large pleiotropic effects affecting ovule development were observed, including abnormal integuments growth and campylotropy, most ovules, however, develop a gametophyte (arrow); DAPI (white, center) and H3K9me2 (green, right) signals.

(C) *nrpd1a-2 nrpd1b-11* ovule. Overlay of DAPI (blue) and H3K9me2 (green) signals.

EC: egg cell; CC: central cell. All images are single optical sections.

Scale bar: 10µm.

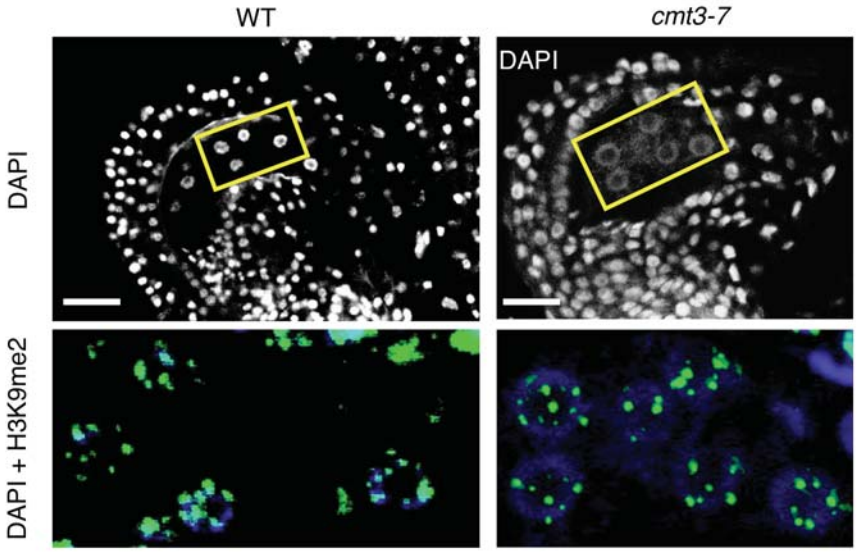

Supplemental Figure 6: H3K9me2 pattern before cellularization in *cmt3-7* mutant plants.
Wild type (WT) and *cmt3-7* immature ovules prior to gametophyte cellularization; whole ovules stained with DAPI (white, single optical sections) and close-ups showing overlays of DAPI (blue) and H3K9me2 (green) signals; projections of consecutive optical sections. Scale bar: 10µm.

Supplemental Table 1: Segregations data in RNAi lines.

Segregation of ovules or seeds with defective and wild type development.

(a) RNAi lines with an arrested central cell phenotype.

(b) RNAi lines with slow-growing endosperm phenotype.

(c) three independent crosses with one RNAi line.

(d) segregation of mature ovules without:with an immunolocalization signal in the central cell when stained with a POLII antibody.

(e) +/-: standard deviation

RNAi lines	Genotype of the transgene	Number of transgenic plants	Segregation Abnormal:WT (e)
pFM1-POLII	+ / -	3	121(+/- 3) : 164 (+/- 20)
pNG-empty	+ / -	3	17(+/- 5) : 200 (+/- 21)
pNG-NG	+ / -	3	150(+/- 15) : 234 (+/- 23)
pNG-POLII (a)	+ / -	4	160(+/- 19) : 244 (+/- 11)
pNG-POLII (b)	+ / -	2	75(+/- 11) : 98 (+/- 15)
pNG-POLII x rdr2	+ / -	3 (c)	88 (+/- 14) : 210 (+/- 15)
pNG-POLII	+ / -	3 (d)	33 (+/- 8) : 39 (+/- 7)

Supplemental Table 2: Mutant lines used in the study.

All mutants were homozygous. The lines were ordered from the Arabidopsis Stock Center or generously provided by the authors of the corresponding references. The *drm1* and *drm2* alleles were provided as a double mutant. The *nrpd1a* and *nrpd1b* alleles were provided as a double mutant. The *dml1*, *dml2* and *dml3* alleles were provided as a triple mutant.

Allele	Gene Name	Locus	Ecotype	Stock#	Reference
rdr2-1	*RDR2*	At4g11130	Col(0)	SAIL-1277H08	(Xie et al., 2004)
kyp-2	*KYP*	At5g13960	L*er*	CS6367	(Jackson et al., 2002)
drm1-1 *drm2-1*	*DRM1* *DRM2*	At5g15380 At5g14620	WS	N6366	(Cao and Jacobsen, 2002)
dme-1S	*DME1*	At5g04560	Col(0)	CS16127	(McElver et al., 2001)
met1-3	*MET1*	At5g49160	Col(0)	N.A.	(Mathieu et al., 2007)
nrpd1a-2 *nrpd1b-1*	*NRPD1a* *NRPD1b*	At1g63020; At2g40030	Col(0)	N.A. SALK_029919	(Pontier et al., 2005)
ros1-3 *dml2-1* *dml3-1*	*ROS1 (DML1)* *DML2* *DML3*	At2g36490; At3g10010; At4g34060	Col(0)	N.A.	(Penterman et al., 2007)
cmt3-7	*CMT3*	At1g69770	L*er*	CS6365	(Lindroth et al., 2004)

Supplemental Table 3: Effect of CMT3 loss-of-function on embryogenesis.

To test for parental effects, we reciprocally crossed homozygous *cmt3-7* plants with wild type plants and examined embryogenesis within the F1 seeds 2 DAP. Self pollinated plants were included as controls. We noted a significant effect of controlled pollinations, which resulted in 8,6% of abnormal embryos in controlled L*er* crosses, as compared to 2,7% in selfed L*er*, Controlling for this factor, the only significant effect was induced by the maternally provided *cmt3-7* allele (*** p<0,01, t-test). The effect of a paternally transmitted allele in controlled pollinations was not significant (ns).

	Genetic Cross		Abnormal F1 Embryos	
Self-Pollinated	Female	Male	%	n
L*er*			2,7	451
cmt3-7			17,6 ***	216
	L*er*	L*er*	8,6	139
	L*er*	*cmt3-7*	11.0 ns	155
	cmt3-7	L*er*	27,5 ***	153
	cmt3-7	*cmt3-7*	19,8 ***	81

Supplemental References:

Cao, X., and Jacobsen, S.E. (2002). Role of the *Arabidopsis* DRM methyltransferases in de novo DNA methylation and gene silencing. Curr Biol **12**, 1138-44.

Jackson, J.P., Lindroth, A.M., Cao, X., and Jacobsen, S.E. (2002). Control of CpNpG DNA methylation by the KRYPTONITE histone H3 methyltransferase. Nature **416**, 556-60.

Lindroth, A.M., Shultis, D., Jasencakova, Z., Fuchs, J., Johnson, L., Schubert, D., Patnaik, D., Pradhan, S., Goodrich, J., and Schubert, I. (2004). Dual histone H3 methylation marks at lysines 9 and 27 required for interaction with CHROMOMETHYLASE3. EMBO J **23**, 4286-96.

Mathieu, O., Reinders, J., Caikovski, M., Smathajitt, C., and Paszkowski, J. (2007). Transgenerational stability of the *Arabidopsis* epigenome is coordinated by CG methylation. Cell **130**, 851-62.

McElver, J., Tzafrir, I., Aux, G., Rogers, R., Ashby, C., Smith, K., Thomas, C., Schetter, A., Zhou, Q., Cushman, M.A., Tossberg, J., Nickle, T., Levin, J.Z., Law, M., Meinke, D., and Patton, D. (2001). Insertional mutagenesis of genes required for seed development in *Arabidopsis thaliana*. Genetics **159**, 1751-63.

Penterman, J., Zilberman, D., Huh, J.H., Ballinger, T., Henikoff, S., and Fischer, R.L. (2007). DNA demethylation in the *Arabidopsis* genome. Proc Natl Acad Sci USA **104**, 6752-7.

Pontier, D., Yahubyan, G., Vega, D., Bulski, A., Saez-Vasquez, J., Hakimi, M.A., Lerbs-Mache, S., Colot, V., and Lagrange, T. (2005). Reinforcement of silencing at transposons and highly repeated sequences requires the concerted action of two distinct RNA polymerases IV in *Arabidopsis*. Genes Dev **19**, 2030-40.

Xie, Z., Johansen, L.K., Gustafson, A.M., Kasschau, K.D., Lellis, A.D., Zilberman, D., Jacobsen, S.E., and Carrington, J. C. (2004). Genetic and functional diversification of small RNA pathways in plants. PLoS Biol **2**, E104.